Journal of
Materials Chemistry A

Accepted Manuscript

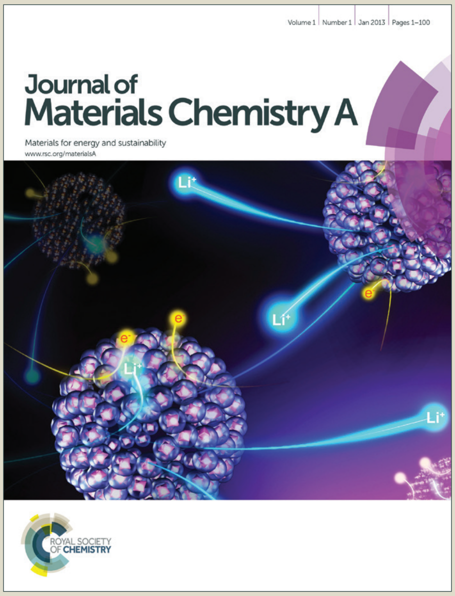

ROYAL SOCIETY
OF **CHEMISTRY**

www.rsc.org/materialsA

Journal of

Materials of Chemistry A

RSCPublishing

COMMUNICATION

Fixing of high soluble Br_2/Br^- in porous carbon as cathode material for rechargeable lithium ion batteries

Cite this: DOI: 10.1039/x0xx00000x

Y. L. Wang,[a] X. Wang,[a] L. Y. Tian,[a] Y. Y. Sun[a] and Shi-hai Ye*[a]

Received 00th January 2012,
Accepted 00th January 2012

DOI: 10.1039/x0xx00000x

www.rsc.org/

LiBr, as a representative of high soluble electrochemical active materials, is fixed in nanopores of conductive carbon black (CCB). The Li/LiBr-CCB battery presents excellent high-rate capability for avoiding the slow solid-phase diffusion of Li ions in traditional solid cathode materials. The success will broaden the range of cathode alternative materials in LIBs and be capable of providing both high power density and energy density.

Rechargeable lithium ion batteries (LIBs) and supercapacitors (SCs), as the most promising portable energy alternative to gasoline, have been rapidly developing during recent decades.[1-5] Some novel energy-storage systems are increasingly attracting great attentions.[6-12] Currently, LIBs and SCs are applied to different fields due to their distinct advantages of high energy density for LIBs and high power density for SCs.[13-15] With the development of LIBs techniques, more and more businesses succeed in applying the traditional LIBs to EVs. However, LIBs units, the power core of EVs, are still facing to huge challenge from environment and cost, especially safety. Moreover, to further fulfil the demand of EV,[16, 17] the power density of LIBs urgently need great development, which is generally one order of magnitude lower than that of SCs,[18-20] because of the slow reaction and mass transfer in the solid electrodes.[21] Additionally, for the traditional solid electrodes in LIBs it is necessary to overcome the lattice barrier while LIBs charging or discharging,[22, 23] which is the slowest step just like "wooden barrel effect".[15, 24] Soluble electrode materials can avoid the slow solid-phase process, implied that the soluble electrode material can greatly enhance the power density of the corresponding batteries. The soluble materials have also been utilized in flow cells in earlier period.[25, 26] Recently, iodide and bromide aqueous solution as active solution have been developed in LIBs.[27-30] However, these batteries still needs a complicated flange-like device to totally separate the catholyte and anolyte. This complex configuration makes it difficult to enter to a broader market, especially to consumer electronics market due to difficulty of miniaturization. Therefore, it is of great significance to utilize soluble materials as electrodes in a traditional LIBs configuration without a complex flange structure. In one of our previous works,[31] the high solubility of active iodine is considered as an obstacle for the stable cycle performance, but the feasibility of soluble electrode in a commercial LIBs configuration is unconsciously and preliminary verified. However, the unstable cycleability, the low energy density resulted from a low voltage plateau and a small theoretical capacity (210 mAh g^{-1}) impedes its further improvement and application. Compared with the I_2/LiI species, the redox pair of Br_2/Br^- has a higher oxidation potential and a lower molecular formula, suggesting that the Li/LiBr has much higher energy density.

Herein, we propose a novel concept: any high soluble redox couple fixed in the nanoporous of porous carbon as one cathode material can be applied in a commercial rechargeable LIBs to achieve much high power density without detraction from the energy density of LIBs. In this manuscript, the Br_2/Br^- redox couple as a representative of high soluble electrochemical active materials, are selected due to its high theoretical capacity (310 mAh g^{-1}) and more positive redox potential. The LiBr/CCB composites are fabricated via dissolution-adsorption method. The designed novel Li/LiBr ultra-batteries are expected to process simultaneously high energy density and power density, capable of taking advantage of both the high energy density of commercial LIBs and the high power density of SCs. Thus, the successful utilization of high soluble electrode materials in a traditional LIBs configuration will broaden the range of cathode alternative materials in LIBs and be capable of providing both high power density and energy density.

The LiBr (Alfa Aesar) and the commercial conductive carbon black (CCB, ketjenblack EC600JD) were dried at 100 °C under vacuum for 24 h before use. LiBr (0.3 g) and CCB (0.7g) were dispersed in ethanol solution (50 ml, 50% v/v) by ultrasonic for 2 h. Then, the mixture was stirred to dry with the stirring rate (150 r/min) at 50°C, and washed with anhydrous ethanol (98.5%, 10 ml) for three times to remove the LiBr on the surface of CCB, then annealed at 200°C for 2 h under Ar.

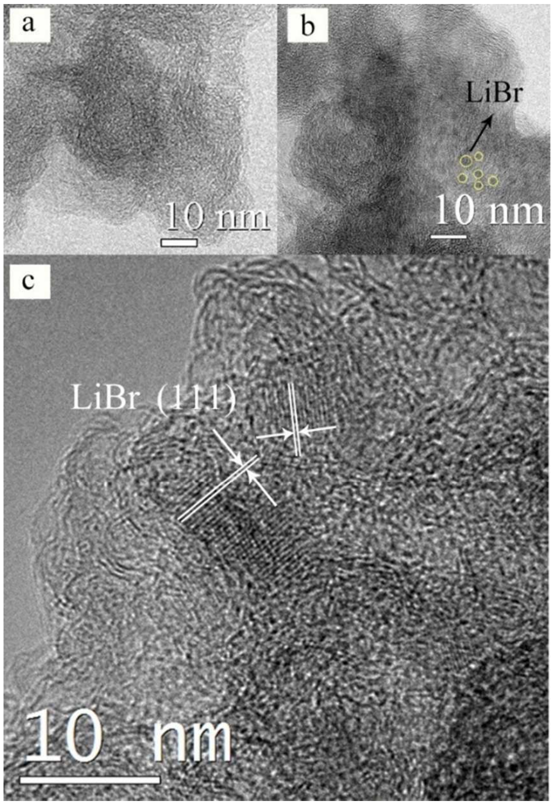

Fig. 1 HRTEM image of the CCB substrate (a); HRTEM images of the as-prepared LiBr-CCB composite (b and c).

LiBr is a soluble salt in both polar and nonpolar solvents. The solubility of LiBr is determined as 0.828 mol L^{-1} in the electrolyte used in test batteries and 1.074 mol L^{-1} in a commercial electrolyte (1M $LiPF_6$ in EC/DMC/EMC with the volumetric ratio of 1:1:1), respectively (First section†). The amount of LiBr in the electrode is unsaturated for the corresponding volume of electrolyte (First section†). The high resolution transmission electron microscope (HRTEM) are employed to analyze the morphology of the conductive carbon black (CCB) substrate and the as-prepared LiBr-CCB composite (Fig. 1). Fig. 1b shows that 2-5 nm particles distribute in the composite. A continuous interference fringe spacing (0.32 nm) can be observed in Fig. 1c, indexed to the lattice plane (111) of LiBr. The scanning electron microscope (SEM) images, corresponding the energy dispersive X-ray spectroscopy (EDX), the high-angle annular dark-field scanning transmission electron microscopy (HAADF-STEM) images and elemental maps of carbon and bromine of CCB and LiBr-CCB samples are carried out (Fig. S4 and S5†). The uniform distribution of the nano-sized LiBr particles in the composite implies that the LiBr active mass should be completely confined in the nanopores of the CCB substrate. Moreover, there are no X-ray diffraction (XRD) peaks of LiBr in the composite, due to the very low volume percentage of LiBr (Fig. S1†). The content of LiBr in the composite is measured as 29.01 wt.% by thermogravimetry analysis (TG) (Fig. S2†). The nitrogen adsorption-desorption experiments also demonstrate that both the surface area and pore volume of CCB decrease after LiBr loading (Fig. S3 and Table S1†).

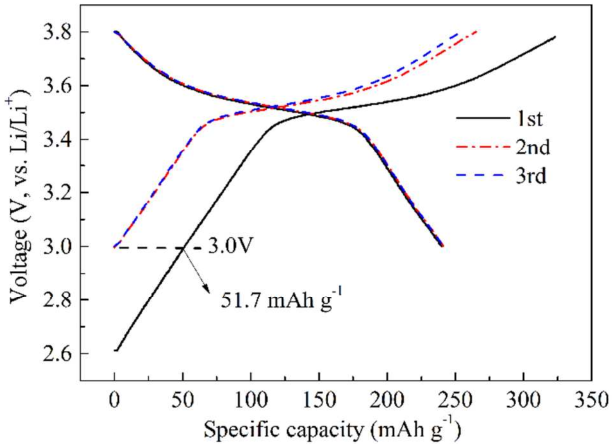

Fig. 2 The charge and discharge profiles in the initial three cycles. The capacity is calculated based on the weight of LiBr in the cathode

The Li/LiBr-CCB batteries are assembled and tested for their electrochemical behavior at the rate of 1C based on the LiBr weight. The charge-discharge curves of the LiBr-CCB composite at the initial three cycle process are presented in Fig. 2. The voltage plateau of charge and discharge is approximately 3.5 V. The initial charge capacity (333.1 mAh g^{-1}) of the LiBr-CCB composite is much higher than the initial discharge capacity (254.6 mAh g^{-1}). The charge capacity at 2.6 - 3.0 V (51.7 mAh g^{-1}) is attributed to capacitive charge of carbon. The initial columbic efficiency can be corrected as 90.5%. The extra charge capacity of 26.8 mAh g^{-1} should be contributed from the surface adsorption rather than the slight "shuttle effect" in the initial 5 cycles.[32] Because the high coulombic efficiency (> 97.0%) in the subsequent cycles means the absence of shuttle effect. During all cycles, the non-active mass (including CCB, acetylene black and polytetrafluorothylene (PTFE)) deliver a cyclic capacity of 66.7 mAh g^{-1} between the voltage region of 3.0 -3.8 V (Fig. S6†). Therefore, subtracted the total capacitive capacity contributed from non-active mass, the charge capacity in the initial 3 cycles devoted by LiBr is respectively about 214.7, 198.5 and 184.7 mAh g^{-1}, corresponding to about 2/3 mole electron reaction of per mole LiBr. It implies that the charged product may be Br_3^- ions. The following charge/discharge cycles exhibit good cycleability. After 100 cycles at the rate of 1C, the discharge capacity remains about 225 mAh g^{-1}, with the capacity retention above 89.5% (Fig. S6†).

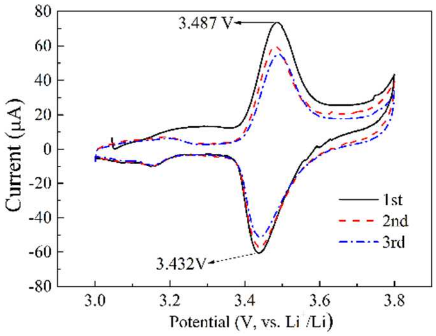

Fig. 3 Cyclic voltammograms of the LiBr-CCB composite at the scan rate of 0.1 mV s^{-1} in the initial 3 cycles.

Cyclic voltammograms (CVs) of the LiBr-CCB composite were measured and illustrated in Fig. 3. The CVs show that a couple of electrochemical redox peaks with good reversibility appear at the potential of 3.5 V, corresponding to the following electrode reactions, shown as Equation 1 and 2.[33] It is in agreement with the charge/discharge voltage plateau in Fig. 2. The two-step oxidation of bromide is described as the bromide ion is first oxidized to the tribromide ion followed by the further oxidation of the tribromide ion to bromine in an organic solution. [33] The oxidation potential is lower than the potential of the Br_2/Br^- redox couple in an aqueous solution.[29] A more positive potential should be necessary to form bromine from tribromide ions in an organic solution because of the very big formation constant of the tribromide ions (the order of magnitude of 10^7) in an organic solution.[34] The electrolyte with wider electrochemical window will help to complete the reaction from bromide ions to bromine in future works.

$$3Br^- - 2e \rightarrow Br_3^- \quad (1)$$

$$Br_3^- + 2e \rightarrow 3Br^- \quad (2)$$

Compared with the traditional solid cathodes in LIBs, the dissolved Br_3^-/Br^- redox couple exhibits a faster kinetic process and a better reversibility. The potential difference between the reduction and oxidation peak potentials is about 55 mV, close to the theoretical value of 59 mV [35]. Its excellent reversibility predicts a good cycling stability and high-rate performance.

In order to reveal the high-rate capability and cycle stability of the LiBr-CCB composite, the cycle performance of the LiBr-CCB battery with various charge-discharge rates is shown in Fig. 4. The capacity of about 240 mAh g^{-1} is retained after the 20th cycle at the low rate of 1 C. As the charge-discharge rate increases to 2 C, 5 C, 10 C, and 20 C, the capacity is still about 220, 210, 200 and 183 mAh g^{-1}, respectively. The high solubility and fast lithium ion kinetic process of the electrode materials lead to excellent rate performance of the LiBr-CCB composite. More importantly, after 100 cycles at various charge-discharge rates, the LiBr-CCB composite restores the discharge capacity of 224.8 mAh g^{-1} at the 1 C rate, same as 224.7 mAh g^{-1} of discharge capacity after 100 cycles always at 1 C (Fig. S6). Therefore, high current density does not harm the cyclability of the composite. Moreover, the excellent cyclic performance demonstrates that the electrochemical reaction process of LiBr can be constrained inside the nanopores of the CCB substrate by strong absorption. Self-discharge performance is investigated after the initial 5 cycles at 1 C. After resting for 7 days, the Li/LiBr-CCB battery still exhibits good discharge capacity and cyclability (Fig. S7†). The detailed charge/ discharge curves before or after resting for 7 days (Fig. S8†) demonstrate that during the 7 days rest time, all the Br_3^- ions fixed in the nanopores of CCB substrate are partly chemically reduced to Br^- ions, partly still fixed in the nanopores of CCB and partly diffused into the bulk of electrolyte. To understand the kinetic of LiBr-CCB composites, electrochemical impedance spectroscopy (EIS) is carried out with an IM6E electrochemical station (Fig. S9†). The fitting data are listed in Table S2† according to the typical equivalent circuit (inset in Fig. S9†). The calculated diffusion coefficient of Li^+ in the electrode system is $1.87*10^{-5}$ cm^2 S^{-1} with a modified EIS method.[36] It is one order of magnitude smaller than that of proton in bulk water ($1.2*10^{-4}$ cm^2 S^{-1}).[37] Furthermore, the fitting Warburg impedance is dozens of ohms only half of the charge transfer impedance. The results imply that diffusion of Li^+ in the whole reaction is very fast, which is distinct from the solid-phase diffusion reaction. Combined with the solubility data of LiBr in the electrolytes it should be reasonable that the dynamic processes of the Br^-/Br_3^- redox in the ultra batteries is a liquid-phase diffusion. Furthermore, the stable cycleability means the electrochemical reaction is fixed in the LiBr-CCB electrode, which may be related to the strong absorbability of nanopores of CCB substrate.

Li/LiBr-CCB ultra batteries include both electrochemical reactions and capacitive charge-discharge processes. During the process of charge, Br^- ions are oxidized to Br_3^- in the CCB substrate and Li^+ ions are reduced to Li at the anode. The oxidized Br_3^- ions are limited in the nanopores of the CCB. This is an electrode reaction. Bis(trifluoromethane)sulfonimide (TFSI) anions move toward the CCB and enter into the double layer of the CCB surface, as Li ions migrate out of the double layer. This process belongs to capacitive charge. Thus, the LiBr-CCB ultra battery combines the redox capacity of the LiBr in the composite and the capacitive characteristics of the nanoporous carbon, allowing for excellent energy density and power density, while the strong absorbability of the carbon nanopores ensures good cycle performance, indicating the feasibility of high soluble electrode material in a traditional LIBs configure.

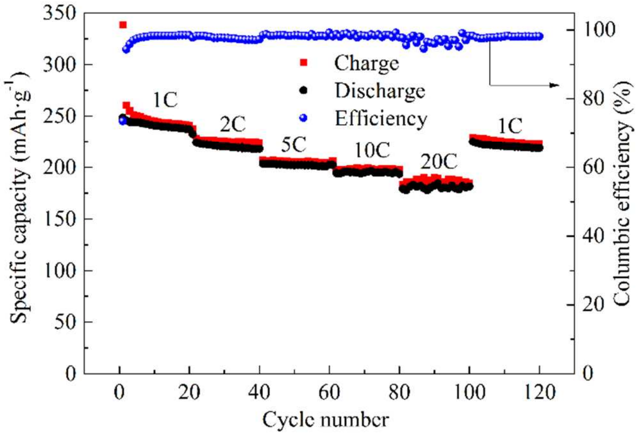

Fig. 4 The cycle performance of LiBr-CCB/lithium cell at various charge-discharge rates. The capacity is calculated based on the weight of LiBr in the composite

In summary, we fabricate the lithium bromide-conductive carbon black composite through heterogeneous nucleation crystallization. The LiBr-CCB composite, combining the strong absorption of porous carbon and the high solubility of LiBr, exhibits a high discharge voltage plateau, high rate capacity, and excellent cycle performance. The excellent high rate charge-discharge performance of LiBr-CCB composite demonstrates that high soluble electrode materials combine the advantages of both the high energy density of LIBs and the high power density of SCs, and thus match the need of EVs and HEVs. The nanoconfined effect of high soluble materials in nanopores and the inhibition of the shuttle effect are the keys to the application in LIBs of these high soluble materials. For the LiBr-CCB composite, the energy density is 275 Wh kg^{-1} with a powder density of 324 W kg^{-1} (1 C), calculated based on the total weight of LiBr-CCB composites. It is not higher than that of commercial cathode materials in LIBs, due to the low loading content of LiBr in the composite. However, the composites still release the energy of 198 Wh kg^{-1} at the power density 6.5 kW kg^{-1} (20 C). It should be mainly attributed to the rapid reaction of liquid-phase Br/Br_3^- redox and high content of CCB in the LiBr-CCB cathode materials, the latter of which could further improve the inner electronic transmission speed of the composite. The energy density of the LiBr-

CCB composites, heavily depending on the content of LiBr in the composite, can be enhanced by synthesizing carbon materials with higher surface area and pore volume. The fixation effect of nanopores of CCB substrate is the key to the success of the rechargeable Li/LiBr battery using the traditional rechargeable LIBs. Given the low cost and high abundance in seawater of elemental bromine and the good electrochemical performance of the composite, ultra batteries, composed of high soluble materials and porous carbon, should be hopeful in playing an important role in the future of chemical storage energy systems. It can be expected that some high soluble redox couple would be utilized as cathode active mass with high power density in LIBs in future. This work based on application of high soluble electrode materials in LIBs should broaden the range of cathode alternative materials in LIBs, especially in term of high power density.

Acknowledgements

We acknowledge financial support from the National Natural Science Foundation of China (51102137 and 21273119), the 973 Program (2015CB251100) and the MOE Innovation Team (IRT13022) of China. We are grateful to Ms. Jacqui Cloud (Colorado school of Mines, US) for polishing the English of the manuscript.

Notes and references

[a] *Institute of New Energy Material Chemistry; Tianjin Key Laboratory of Metal and Molecule Based Material Chemistry; Synergetic Innovation Center of Chemical Science and Engineering (Tianjin), Nankai University, Weijin Road, No.94, Tianjin, 300071, China. Email: yeshihai@nankai.edu.cn Fax/Tel:+86-22-23502604*

† Electronic Supplementary Information (ESI) available: Experimental details and additional figures and tables. See DOI: 10.1039/c000000x/

1. P. G. Bruce, B. Scrosati and J. M. Tarascon, *Angew. Chem.-Int. Edit.*, 2008, **47**, 2930-2946.
2. B. C. Melot and J. M. Tarascon, *Acc. Chem. Res.*, 2013, **46**, 1226-1238.
3. N.-S. Choi, Z. Chen, S. A. Freunberger, X. Ji, Y.-K. Sun, K. Amine, G. Yushin, L. F. Nazar, J. Cho and P. G. Bruce, *Angew. Chem., Int. Ed.*, 2012, **51**, 9994-10024.
4. Y. Hu and X. Sun, *J. Mater. Chem. A*, 2014, **2**, 10712-10738.
5. Y. B. Tan and J.-M. Lee, *J. Mater. Chem. A*, 2013, **1**, 14814-14843.
6. J. F. Qian, Y. Xiong, Y. L. Cao, X. P. Ai and H. X. Yang, *Nano Lett.*, 2014, **14**, 1865-1869.
7. Y. Wang, J. Yi and Y. Xia, *Adv. Energy Mater.*, 2012, **2**, 830-840.
8. M. Park, H. Sun, H. Lee, J. Lee and J. Cho, *Adv. Energy Mater.*, 2012, **2**, 780-800.
9. G. C. Li, G. R. Li, S. H. Ye and X. P. Gao, *Adv. Energy Mater.*, 2012, **2**, 1238-1245.
10. K. Xi, P. R. Kidambi, R. Chen, C. Gao, X. Peng, C. Ducati, S. Hofmann and R. V. Kumar, *Nanoscale*, 2014, **6**, 5746-5753.
11. N. Mahmood, C. Zhang, H. Yin and Y. Hou, *J. Mater. Chem. A*, 2014, **2**, 15-32.
12. Y. Z. Zhang, S. Liu, G. C. Li, G. R. Li and X. P. Gao, *J. Mater. Chem. A*, 2014, **2**, 4652-4659.
13. M. Armand and J. M. Tarascon, *Nature*, 2008, **451**, 652-657.
14. A. G. Pandolfo and A. F. Hollenkamp, *J. Power Sources*, 2006, **157**, 11-27.
15. J. Wang and X. Sun, *Energy Environ. Sci.*, 2012, **5**, 5163-5185.
16. A. A. Pesaran, National Renewable Energy Laboratory, 2011.
17. M. Al Sakka, H. Gualous, N. Omar and J. Van Mierlo, in *New Generation of Electric Vehicles*, ed. Z. Stevic, 2012.
18. X. P. Gao and H. X. Yang, *Energy Environ. Sci.*, 2010, **3**, 174-189.
19. D. Liu and G. Cao, *Energy Environ. Sci.*, 2010, **3**, 1218-1237.
20. J. T. Zhang, S. Liu, G. L. Pan, G. R. Li and X. P. Gao, *J. Mater. Chem. A*, 2014, **2**, 1524-1529.
21. J. Jiang, Y. Li, J. Liu, X. Huang, C. Yuan and X. W. Lou, *Adv. Mater.*, 2012, **24**, 5166-5180.
22. Y. Ren, A. R. Armstrong, F. Jiao and P. G. Bruce, *J. Am. Chem. Soc.*, 2009, **132**, 996-1004.
23. X.-L. Wu, L.-Y. Jiang, F.-F. Cao, Y.-G. Guo and L.-J. Wan, *Adv. Mater.*, 2009, **21**, 2710-2714.
24. L. Mai, H. Li, Y. Zhao, L. Xu, X. Xu, Y. Luo, Z. Zhang, W. Ke, C. Niu and Q. Zhang, *Sci. Rep.*, 2013, **3**, 1-8.
25. M. Bartolozzi, *J. Power Sources*, 1989, **27**, 219-234.
26. E. Sum and M. Skyllas-Kazacos, *J. Power Sources*, 1985, **15**, 179-190.
27. Y. Zhao, L. Wang and H. R. Byon, *Nat. Commun.*, 2013, **4**, 1896.
28. Y. Zhao, M. Hong, N. B. Mercier, G. H. Yu, H. C. Choi and H. R. Byon, *Nano Lett.*, 2014, **14**, 1085-1092.
29. Y. Zhao, Y. Ding, J. Song, L. Peng, J. B. Goodenough and G. Yu, *Energy Environ. Sci.*, 2014, **7**, 1990-1995.
30. Z. Chang, X. Wang, Y. Yang, J. Gao, M. Li, L. Liu and Y. Wu, *J. Mater. Chem. A*, 2014, **2**, 19444-19450.
31. Y. L. Wang, Q. L. Sun, Q. Q. Zhao, J. S. Cao and S. H. Ye, *Energy Environ. Sci.*, 2011, **4**, 3947-3950.
32. A. Kaya and A. Schumpe, *Chem. Eng. Sci.*, 2005, **60**, 6504-6510.
33. W. K. Behl, *J. Electrochem. Soc.*, 1989, **136**, 2305-2310.
34. I. V. Nelson and R. T. Iwamoto, *J. Electroanal. Chem.*, 1964, **7**, 218-221.
35. A. J. Bard and L. R. Faulkner, *Electrochemical Methods: Fundamentals and Applications*, Wiley, New York, 2001.
36. P. Yu, B. N. Popov, J. A. Ritter and R. E. White, *J. Electrochem. Soc.*, 1999, **146**, 8-14.
37. M. Gutman, E. Nachliel and S. Moshiach, *Biochemistry*, 1989, **28**, 2936-2940.

Fixing of high soluble Br_2/Br^- in porous carbon as cathode material for rechargeable lithium ion batteries

Y.L. Wang, X. Wang, L. Y. Tian, Y. Y. Sun, and S. H. Ye*

Graphical abstract